

Journal Pre-proof

The Generation of Hydroxyl Radicals and Electro-oxidation of Diclofenac on Pt-doped SnO₂-Sb electrodes

Maribel G. Fernández-Aguirre, Raúl Berenguer, Samuel Beaumont, Montserrat Nuez, Adolfo La Rosa-Toro, Juan Manuel Peralta-Hernández, Emilia Morallón

PII: S0013-4686(20)31079-3

DOI: <https://doi.org/10.1016/j.electacta.2020.136686>

Reference: EA 136686

To appear in: *Electrochimica Acta*

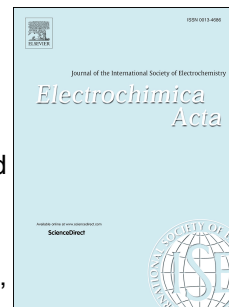
Received Date: 28 April 2020

Accepted Date: 22 June 2020

Please cite this article as: M.G. Fernández-Aguirre, R. Berenguer, S. Beaumont, M. Nuez, A. La Rosa-Toro, J.M. Peralta-Hernández, E. Morallón, The Generation of Hydroxyl Radicals and Electro-oxidation of Diclofenac on Pt-doped SnO₂-Sb electrodes, *Electrochimica Acta*, <https://doi.org/10.1016/j.electacta.2020.136686>.

This is a PDF file of an article that has undergone enhancements after acceptance, such as the addition of a cover page and metadata, and formatting for readability, but it is not yet the definitive version of record. This version will undergo additional copyediting, typesetting and review before it is published in its final form, but we are providing this version to give early visibility of the article. Please note that, during the production process, errors may be discovered which could affect the content, and all legal disclaimers that apply to the journal pertain.

© 2020 Elsevier Ltd. All rights reserved.



The Generation of Hydroxyl Radicals and Electro-oxidation of Diclofenac on Pt-doped SnO₂-Sb electrodes

Maribel G. Fernández-Aguirre^{a,b}, Raúl Berenguer^a, Samuel Beaumont^a, Montserrat Nuez^a, Adolfo La Rosa-Toro^b, Juan Manuel Peralta-Hernández^c, Emilia Morallón^a

^a *Instituto Universitario de Materiales and Departamento de Química Física. Universidad de Alicante. Apartado 99. E-03080 Alicante (Spain)*

^b *Escuela Profesional de Química, Facultad de Ciencias, Universidad Nacional de Ingeniería, Av. Túpac Amaru, 210, Lima (Peru)*

^c *Department of Chemistry, Universidad de Guanajuato (Mexico)*

Abstract

Pt-doped SnO₂-Sb electrodes constitute promising candidates for the electrochemical abatement of refractory pollutants, but their efficacy to oxidize emerging pollutants remains uncertain. In this work, the electrochemical oxidation of diclofenac, pharmaceutical pollutant, on Pt-doped Ti/SnO₂-Sb electrodes has been studied by cyclic voltammetry and galvanostatic treatment in neutral medium. In parallel, the capability of these anodes to generate hydroxyl radicals ([•]OHs) has been analysed by in-situ UV spectroelectrochemical measurements. For comparison purposes, the responses of Ti/SnO₂-Sb and commercial Ti/Pt and BDD anodes were also evaluated. The voltammetric and electrolysis results show that the different Ti/SnO₂-Sb anodes can effectively oxidize and mineralize diclofenac, so their electrochemical activity lies in between that of Ti/Pt and BDD. The incorporation of small amounts of Pt (3-13 at.%) into the SnO₂-Sb coatings, despite hindering the [•]OHs generation, enhances the kinetics and efficiency for diclofenac oxidation and mineralization. This better overall response is attributed to a synergy between diclofenac-Pt interaction and efficient [•]OHs generation. Pt-doped Ti/SnO₂-Sb electrodes are then presented as a cheaper potential alternative to BDD for treating pharmaceuticals pollutants in waters.

Keywords: electrocatalysis; anodic oxidation; Tin dioxide electrodes; hydroxyl radicals; diclofenac removal

29 **Corresponding author:**

30 Raul Berenguer

31 raul.berenguer@ua.es

32 Telf. 34-965909150

33 Fax: 34-96590 3464

34

Journal Pre-proof

35 **1. Introduction**

36 Diclofenac, a nonsteroidal anti-inflammatory, analgesic, and antipyretic drug, is one of the most
37 widely available pharmaceuticals worldwide [1]. Considering the continued release, biodegradation
38 resistance and persistence [2-7], and/or toxic effects [8-11] of diclofenac, it is necessary to develop
39 new methodologies for its elimination.

40 Various technologies have been proposed and reviewed for the removal of diclofenac [2,12-16].
41 Based on the generation of physisorbed hydroxyl radicals ($\cdot\text{OHs}$), the anodic oxidation of pollutants
42 constitutes probably the simplest advanced oxidation process (AOP) [17-20] and, thus, one of the
43 most promising methods for the degradation of this drug [21]. This technology gathers several
44 advantages to remove toxic biorefractory organic compounds [22]. However, its feasible application
45 relies on the nature of the anode, which determines the efficiency and selectivity of the oxidation
46 process, and the cost and durability [17-20,23].

47 To now, there are few studies on the anodic oxidation of diclofenac and most of them have been
48 carried out with the Boron-Doped Diamond (BDD) anode [24-27], demonstrating its capability to
49 full mineralization and toxicity reduction. Despite its good performance, the practical utilization of
50 the BDD is limited by its high cost and fragility (because it is generally supported as a thin film on
51 silicon wafers). On the other hand, other electrodes, like Pt [25,28], PbO_2 [27] and carbon materials
52 [24,28], were also investigated for diclofenac oxidation.

53 Exhibiting a high overpotential for the oxygen evolution reaction (OER), non-active $\text{SnO}_2\text{-Sb}$ anodes
54 constitute a promising cheaper and efficient alternative for the electro-oxidation of pollutants
55 [17,29,30]. It was found that the incorporation of a small percentage of Pt (3-13 metal atomic percent
56 (at.)) remarkably increases their short service life [31,32] and their catalytic activity for phenol
57 degradation [33,34] in different electrolytes. Hence, both fundamental and practical studies on the
58 electrocatalytic properties and potential applicability of these anodes have aroused great interest.

59 It is generally assumed that the performance of a given anode towards the electrochemical abatement
60 of organic pollutants is correlated with its capability to generate oxidizing $\cdot\text{OHs}$. Then, considering
61 the observed catalytic effects of Pt [33,34], a promotion of $\cdot\text{OHs}$ generation would be expected by
62 incorporating Pt into the $\text{SnO}_2\text{-Sb}$ anodes. Nevertheless, in a recent study [35] the electrocatalytic
63 effect of Pt has been associated to a strong specific adsorption of phenol on Pt/PtOx sites. Despite
64 this controversy, the influence of Pt doping on the capability of $\text{SnO}_2\text{-Sb}$ anodes to produce $\cdot\text{OHs}$ has
65 been never investigated. Moreover, the catalytic activity of Pt-doped or undoped $\text{SnO}_2\text{-Sb}$ anodes for
66 the electro-oxidation of diclofenac has been never explored.

67 This work presents a study on the electrocatalytic activity of various Ti/ $\text{SnO}_2\text{-Sb}$ anodes towards the
68 generation of $\cdot\text{OHs}$ and the oxidation and mineralization of diclofenac, as one of the most important
69 pharmaceuticals, in neutral medium. The effect of the Pt content on the $\text{SnO}_2\text{-Sb}$ coating is
70 investigated. For comparison purposes, the performance of Ti/Pt and BDD commercial anodes has
71 been also analyzed. Considering that the anodic removal of diclofenac is a complex reaction,
72 involving various concurrent electrochemical processes, the catalytic activity of the different anodes
73 was studied by different techniques, such as cyclic voltammetry (CV), in-situ UV
74 spectroelectrochemical measurements and galvanostatic electrolysis, and by using different fixed
75 electrochemical conditions.

76 These conditions were selected with the intention of better discerning the electrocatalytic response of
77 the electrodes, without optimization of the experimental conditions.

78

79 **2. Experimental**

80 In the course of diclofenac removal by anodic treatment, three main electrochemical processes may
81 occur simultaneously on the electrode surface: (i) the direct oxidation without mediation of $\cdot\text{OHs}$; (ii)
82 the mediated oxidation involving the generation of $\cdot\text{OHs}$; and (iii) the OER. Thus, in order to provide
83 a comprehensive picture of the electrocatalytic activity of the electrodes, these coupled processes

84 were studied concurrently and separately. The first two reactions have been individually studied by
85 CV and in-situ UV spectroelectrochemical measurements, respectively. Studies on the OER were
86 previously reported [31,32,36]. The complex reaction, diclofenac removal, was investigated by
87 galvanostatic electrolysis. It is noteworthy to remark, then, that the electrochemical conditions used
88 to better decouple the processes in CV and in-situ UV techniques were different and, therefore, did
89 not try to be representative of those of the galvanostatic removal of diclofenac.

90 **2.1. Electrode materials**

91 Antimony and/or platinum doped tin oxide electrodes were prepared in our lab by conventional
92 thermal decomposition of the salt precursors ($\text{SnCl}_4 \cdot 5\text{H}_2\text{O}$ (Aldrich), SbCl_3 (Fluka) and H_2PtCl_6
93 (Aldrich) in acidified absolute ethanol (J.T. Baker) onto Ti substrate in the form of mesh or plate
94 (INAGASA S.A.). The composition and nomenclature of the studied electrodes was Ti/ SnO_2 -Sb-
95 Pt(x%), with Sb = 13 at% and x = 3 and 13 at% Pt (metal atomic composition); the Ti/ SnO_2 -Sb
96 electrode without Pt has been also studied. Details on the preparation and physico-chemical
97 properties of this type of electrodes can be found in the literature [31,34-38]. The Ti/Pt mesh
98 (INAGASA S.A.) and BDD (Si/BDD, Adamant Technologies) plate electrodes were commercially
99 supplied. Prior the electrochemical measurements, all the electrodes (plates or meshes) were
100 submitted to a galvanostatic pre-treatment at 10 mA/cm^2 for 5 min to clean and stabilize the surface.

101

102 **2.2. Electrochemical behavior towards diclofenac oxidation. Cyclic voltammetry**

103 The electrocatalytic response of the different electrodes towards diclofenac oxidation was studied by
104 cyclic voltammetry. Moreover, a polycrystalline Pt electrode with well-known electrochemical
105 features, was used as model electrocatalyst to study the interaction of Pt with diclofenac. Prior usage,
106 the surface of this electrode was thermally cleaned and subsequently protected from the laboratory
107 atmosphere by a droplet of ultrapure water of $18.2 \text{ M}\Omega \text{ cm}$ obtained from a Milli-Q[®] Advantage A10
108 water purification system (Merck Millipore).

109 The voltammetric measurements were performed in a conventional glass-made three-electrode cell
110 by using a VSP Biologic potentiostat (Bio-logic Science Instruments). 0.5 M Na₂SO₄ (Merck p.a.)
111 solutions, without or with 200 ppm sodium diclofenac (Sigma-Aldrich, molecular weight 318.1
112 g/mol), were prepared with ultrapure water and used as electrolyte. Since dissolved O₂ can affect the
113 voltammetric response of the anodes, especially when containing Pt species, the solutions were
114 degassed by N₂ bubbling for 20 min prior characterization. A Pt wire and an Ag/Ag/Cl(3 M KCl)
115 electrode immersed in the same solution were used as counter and reference electrodes, respectively.
116 A constant scan rate of 50 mV s⁻¹ was used to record the cyclic voltammograms and the current
117 densities were calculated by using the geometric area of the electrodes immersed in the electrolyte (2
118 cm² for all the electrodes, instead of 1 cm² for the BDD anode.
119 The voltammetric charge associated to diclofenac oxidation prior the OER (Q_{oxid}/Q_{blank}) was used in
120 this work to quantitatively estimate the capability/affinity of the different anodes for the direct (non-
121 •OH-mediated) oxidation of diclofenac [33,39]. This charge was calculated by integrating the
122 positive current in the potential range where the signal in the presence of diclofenac overpasses that
123 of the blank experiment without diclofenac (Q_{oxid}), and normalizing by the charge of the blank
124 experiment (Q_{blank}), within the same potential range, to correct the contribution of a variant electrical
125 double-layer (see details in the Figure S1 of the supporting information, SI).

126

127 **2.3. Electrolysis runs**

128 The capability of the different electrodes to electrochemically abate diclofenac was explored by
129 using galvanostatic experiments in an undivided filter-press cell, with a plane electrode area of 20
130 cm², operated in batch recirculation. A volume of 200 cm³ of 200 ppm diclofenac + 0.5 M Na₂SO₄
131 aqueous solution was continuously pumped through the cell and a jacketed reservoir for temperature
132 control at 298 K during the experiment. The aqueous solutions were made up with distilled water.
133 The different electrodes in the form of expanded meshes and the BDD plate were used as anodes and

134 a stainless steel (310L) plate acted as cathode in all the experiments. A constant current of 1 A
 135 (current density = 50 mA cm⁻²) was applied for 5 h of electrolytic treatment and different aliquots
 136 were taken as a function of time to follow the extent diclofenac degradation. This current density
 137 value was arbitrarily chosen to get a meaningful comparative response of the electrodes within the
 138 5h-experiments.

139 The concentration and transformation of diclofenac was monitored by UV-vis absorption
 140 spectroscopy (Jasco V-670 UV-vis-NIR spectrometer) over the wavelength range of 200-400 nm
 141 (see the calibration data in the Figure S2 of the SI) and the total organic carbon (TOC) was measured
 142 in a TOC Analyser (Shimadzu). Moreover, the electrode potential of the anodes was followed by
 143 using an Ag/AgCl/3M KCl reference electrode externally connected with a luggin capillary. Respect
 144 to the electrolyte, no significant changes on the solution pH were identified during the electrolytic
 145 experiments (see section 3.3.), so pH monitoring or the use of a buffer were considered unnecessary.
 146 The efficiency of the anodes for diclofenac oxidation (Eff_{Diclof} , in %) and TOC removal (Eff_{TOC} ,
 147 in %) have been calculated according to the following equations:

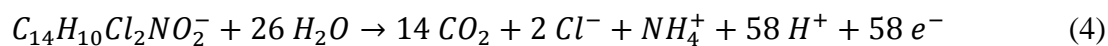
$$148 \quad Eff_{Diclof} = \frac{[Diclof]_f - [Diclof]_0}{[Diclof]_0} \times 100 \quad (1)$$

$$149 \quad Eff_{TOC} = \frac{[TOC]_f - [TOC]_0}{[TOC]_0} \times 100 \quad (2)$$

150 where f and 0 refer to the final and initial concentrations, respectively, of diclofenac and TOC. The
 151 mineralization current efficiency (MCE , in %) at a given time (t , in s) was calculated by using the
 152 following equation:

$$153 \quad MCE = \frac{n F V \Delta(TOC)}{m I t} \times 100 \quad (3)$$

154 where F is the Faraday constant (96485 C mol⁻¹), V is the solution volume (L), $\Delta(TOC)$ is the TOC
 155 decay at a given time ($[TOC]_t - [TOC]_0$, in g L⁻¹), m is the number of carbon atoms per molecule of
 156 diclofenac (14 C atoms), I is the applied current (A), and n is the number of electrons consumed for
 157 the mineralization of one molecule of diclofenac assuming the following reaction [25]:



2.4. Generation of hydroxyl radicals

The determination of the $\cdot OH$ s was carried out spectrophotometrically by means of the reaction with N,N-dimethyl-p-nitrosoaniline (RNO), used as radical scavenger, at constant potential [40,41]. The method is based on the direct relationship between the generation of the $\cdot OH$ radicals and the depletion of the RNO concentration (RNO bleaching), which can be followed by UV spectroscopy. To do that, a conventional UV cell was adapted to become a three-electrodes electrochemical cell for in-situ UV electrochemical degradation of RNO (Figure 1a). The counter electrode (CE) was a Pt wire and a wire of Ag acted as pseudo-reference electrode (RE), whereas the studied anodes were used as working electrode (WE) with a exposed geometric area of 2 cm², instead for the BDD, working with 1 cm². A calibration curve was made before the experimental series by following the dependence of the absorbance band at $\lambda = 440$ nm of RNO with its concentration in a range of 2-50 μM (see Figure S3 in the SI).

Figure 1b depicts the experimental set-up used for the electrochemical measurements. Each WE was allocated into the electrochemical cell containing a 20 μM RNO aqueous solution, and checking that the submerged electrodes do not block the pathway of the light beam. Then the cell was placed inside a UV-Vis-NIR JASCO V-670 spectrophotometer and connected to an Orignalys OrigaFlex500 Potentiostat-galvanostat. The external connecting wires were passed through the equipment dark chamber door without letting the external light to enter.

Before starting the electrochemical experiments, a UV spectrum was measured between 600 and 200 nm (labelled as 0 min) to check the initial conditions of the RNO solution, ruling out any potential degradation of this compound during the time stored. In this sense, if the starting band absorbance of the used RNO solution deployed more than 3% from the controlled expected one, a new solution was prepared to start the experiment.

183 Once checked, a chronoamperometric method was programmed to the potentiostat by the
184 Origamaster software. A constant potential of 1.7 V (vs. Ag/AgCl/3M KCl) was settled to be applied
185 for 2 hours, taking a UV spectrum every 2 minutes during the first 10 minutes, and thereafter every
186 10 minutes. This potential was selected because it is above (but not far from) the onset of the OER
187 on the different Ti/SnO₂-Sb (without and with Pt) and Ti/Pt anodes (see below Figure 2). Larger
188 potentials could be detrimental for this experiment because of the promotion of the OER [42] and/or
189 direct and over-oxidation of RNO. In the case of BDD, a higher constant potential of 2.4 V (vs.
190 Ag/AgCl/3M KCl) was also tested. The resulting spectra were recorded in the PC by the Spectra
191 Manager™ software. All the solutions used for calibration and electro-oxidation of RNO were
192 prepared with ultrapure water. Moreover, additional experiments were performed also at constant
193 current (from 5 to 50 mA/cm²) to confirm the trends found potentiostatically. Nevertheless, these
194 experiments were necessarily performed ex-situ because of the constraints caused by strong bubbling
195 in the in-situ set up.

196

197 **3. Results and Discussion**

198 **3.1. Cyclic Voltammetry**

199 The electrochemical behavior of diclofenac on the different electrodes was studied by cyclic
200 voltammetry. This analysis mainly encompassed the relatively low potentials prior (and therefore
201 excluding) the OER, thus, it enabled to decouple and study diclofenac interaction and oxidation on
202 the anode surface in the absence of [•]OHs.

203 Figure 2 compares the voltammetric responses of the studied electrodes in the absence and presence
204 of diclofenac. Respect to commercial anodes, the negligible oxidation currents observed for Ti/Pt in
205 the presence of diclofenac (Figure 2a), resulting in a normalized oxidation charge (Q_{oxid}/Q_{blank}) close
206 to 1 (Table 1), was indicative of a poor catalytic response. However, two clear oxidation processes
207 were discerned for BDD (Figure 2b). In agreement with literature, the first process at ca. 0.95 V may

208 be associated to the direct electro-oxidation of diclofenac on the surface of BDD [23,43-46]; while
209 the sharp current rise from 1.50 V, towards the potential range where the OER takes place (see the
210 voltammogram of BDD anode in the blank electrolyte), might involve the $\cdot\text{OH}$ s-mediated oxidation
211 of diclofenac. The calculated $Q_{\text{oxid}}/Q_{\text{blank}}$ for these processes was remarkably high, ca. 21, entailing a
212 superb activity for diclofenac oxidation.

213 For the Ti/SnO₂-Sb electrode without Pt (Figure 2c), an anodic current rise is observed above 0.5 V
214 in the presence of diclofenac. Because it starts at ca. 1 V below the onset of the OER, this process
215 may be attributed to the direct (non- $\cdot\text{OH}$ mediated) electro-oxidation of adsorbed and/or solution
216 diclofenac. Such a direct oxidation has been also observed on other metal oxide anodes [47-49].
217 Moreover, the diclofenac oxidation current increased with the augment of Pt content in the Pt-doped
218 Ti/SnO₂-Sb electrodes (Figures 2d and 2e). Thus, the normalized oxidation charge ($Q_{\text{oxid}}/Q_{\text{blank}}$) for
219 the electrode without Pt (1.45) increased up to ca. 1.7 and 1.8 for the electrodes with 3 and 13 at.%
220 Pt, respectively (Table 1).

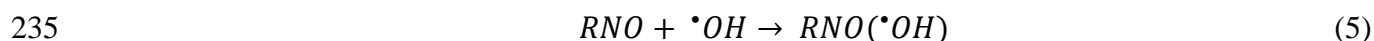
221 Given the remarkable activity observed by polycrystalline Pt (see Figure S4 in the SI), the obtained
222 results are attributed to a significant interaction and oxidation activity of diclofenac on the Pt present
223 in the Ti/SnO₂-Sb electrodes. Discrepancies with the case of Ti/Pt may be explained by the different
224 properties of Pt in these electrodes, prepared by completely distinct methods, which greatly affect the
225 electrocatalytic activity of Pt catalysts [50] (see further discussion in the SI).

226

227 **3.2. Generation of hydroxyl radicals**

228 The capability of the different electrodes to generate hydroxyl radicals was related to the kinetics of
229 RNO bleaching followed by in-situ electrochemical UV spectroscopy. The evolution of current
230 density during the potentiostatic experiments can be found in the SI (Figure S5). The absorbance at
231 the wavelength of the maximum, i.e. the concentration of RNO, started to decrease after applying the
232 constant potential of 1.7 V on all the different tested anodes (see as example the spectra of the

233 different Ti/SnO₂-Sb anodes in Figures 3a-c, and those of the other electrodes in Figure S6 of the SI),
 234 according of the following reaction:



236 The concentration of RNO at a given time ([RNO]) was then calculated with the calibration curve. It
 237 was observed that, in all cases, the variation of RNO concentration followed an exponential-like
 238 decay, so it was fitted to a pseudo-first order kinetics according to the expression:

$$239 \quad \ln \frac{[RNO]}{[RNO]_0} = -k_{app} \cdot t \quad (6)$$

240 where [RNO]₀ and [RNO] are the initial and time-dependent concentrations of RNO, and *k_{app}* refers
 241 to the apparent first-order rate constant for RNO concentration decay (*k_{app}* = [$\cdot OH$] · *k*, assuming a
 242 constant “pseudo steady-state” concentration of $\cdot OH$ s during the measurements). Considering that (i)
 243 the reaction rate of RNO with $\cdot OH$ s is very fast (ca. 1.25 × 10¹⁰ M⁻¹ s⁻¹); (ii) the bleaching of RNO is
 244 very selective to oxidation by $\cdot OH$ s; and (iii) the (direct) non- $\cdot OH$ -mediated oxidation of RNO may
 245 be negligible, as reported in previous works (see the references [17,40-42]); hence, the rate constant
 246 for RNO concentration (*k_{app}*) decay may approximate that for $\cdot OH$ s generation (*k_{app}*($\cdot OH$)).

247 The logarithm of the normalized RNO concentration was plotted versus the reaction time (Figure
 248 3d). As observed in the figure, in all cases the experimental data followed a straight trend with R² >
 249 0.99, validating the proposed kinetic model [41,42]. The apparent rate constants for $\cdot OH$ s generation
 250 on the different anodes were deduced from the slope of these kinetic plots and are collected in Table
 251 1, and the current densities passing through the different anodes follow the same trend (Fig. S5). As
 252 it can be observed, at 1.7 V the fastest generation of $\cdot OH$ s was observed on the Ti/SnO₂-Sb and BDD
 253 anodes with apparent rate constants of 0.0130 and 0.132 min⁻¹, respectively. These results agree with
 254 literature, which generally attributes a higher capability to produce $\cdot OH$ s to non-active anodes [17-
 255 20,23]. Nevertheless, it is worthy to mention that the geometric area of the BDD was the half that of
 256 the Ti/SnO₂-Sb. Moreover, it can be inferred that 1.7 V, the potential used for comparison, is not a
 257 too high potential for BDD. Thus, a spectroelectrochemical test of BDD carried out at 2.4 V (vs.

258 Ag/AgCl/Cl⁻(3M)) showed that the rate constant considerably increased to 0.0161 min⁻¹ (Table 1).
259 On the contrary, Ti/Pt exhibited the slowest rate for [•]OH generation (Table 1) [51]. This result is in
260 line with the comparatively poorer performance of this anode to electro-oxidize refractory organics
261 [17,20].

262 The incorporation of Pt into the SnO₂-Sb anode decreases the rate constants for [•]OH generation
263 (Table 1). This is a new interesting result that cannot be expected from the literature, since Pt doping
264 was found to thermodynamically and kinetically promote the OER [35,36], and the electrocatalytic
265 activity towards organics oxidation [33-35]. Considering the mechanism proposed by Comninellis et
266 al. [17], which regards the [•]OHs as reaction intermediates for both the OER and organic oxidation,
267 and the changes on k_{app} observed in this work, it is hypothesized that the presence of Pt may alter
268 (weaken) the physisorption strength of [•]OHs (reduce the potential needed) to form O₂ or react with
269 organic molecules, but not the rate of [•]OH formation (water discharge). In other words, the
270 promotion and acceleration of OER and/or organic oxidation induced by Pt may come from
271 destabilization of surface-[•]OHs, instead of a faster [•]OHs generation. This agrees with the true
272 electrocatalytic effects observed for Pt doping on the OER and phenol electro-oxidation [35].

273 The found trend in [•]OHs generation rate over the different anodes was confirmed by carrying the
274 experiments at different constant current densities, observing larger differences in reaction rates at
275 higher current densities (figures not shown). Nevertheless, these experiments did not enable to
276 calculate accurate rate constants because of a promoted OER [42].

277

278 3.3. Electrolysis performance

279 Finally, the response of the different electrodes to electro-oxidize diclofenac was also tested under
280 galvanostatic conditions in a flow electrochemical filter-press cell. The diclofenac concentration was
281 followed by UV spectroscopy. Figure 4 depicts the evolution of the diclofenac absorption band
282 centered at 275 nm during the electrolytic experiments with the different electrodes.

283 In all cases, it is observed that the absorption band progressively decreases with time, without any
284 shift of its position. Considering the strong effect of pH on the wavelength of the maximum
285 absorption of diclofenac in UV spectra, this experimental fact may be indicative of non-significant
286 changes on pH during electrolysis. Thus, while the anodic processes generate protons the cathodic
287 ones produce base, so that the bulk pH remain neutral. Nevertheless, the oxidation of diclofenac
288 might occur in an acid local environment, the local pH depending on the current density. Moreover,
289 other bands are not formed during the course of the electrolysis, indicating that the generated by-
290 products from diclofenac oxidation do not seem to interfere the UV analysis of diclofenac.

291 Figure 5a represents the calculated diclofenac concentration versus electrolysis time. The generally
292 observed decay in diclofenac concentration pointed out that all the tested electrodes were effective to
293 electro-oxidize diclofenac. Furthermore, the parallel decrease in TOC (Figure 5b), together with
294 negligible variations in the total inorganic carbon, revealed that all the anodes can also mineralize
295 this compound. The efficiencies for diclofenac oxidation and TOC removals were determined from
296 the initial and final diclofenac and TOC concentrations, respectively, and are listed in Table 1. In
297 addition, Table 1 also collects the calculated values for the mineralization current efficiency (MCE).
298 These values did not exceed 10 % even for the most effective BDD anode. Nevertheless, it is
299 important to remark that the optimization of neither the electrochemical variables nor current
300 efficiencies was attempted in this work.

301 Respect to the concentration decays, they first followed a linear trend and became exponential after
302 ca. 1 h of experiment. These regimes were initially envisioned by the kinetic model of Comninellis et
303 al. [18,20,44,45] for the electrochemical combustion of organics on ideally non-active BDD, and
304 observed also for the electro-oxidation of phenol on different metal oxides including Pt-doped SnO₂-
305 Sb [34]. Details of the model applied for BDD and its derivation for non-ideal non-active electrodes
306 can be found in these last references. Then, the concentration decays during the first hour of
307 experiments were fitted to a pseudo zero-order kinetics:

$$308 \quad [Diclof] = [Diclof]_0 - k_o t \quad (7)$$

309 and

$$310 \quad TOC = TOC_0 - k'_0 t \quad (8)$$

311 while the data within 1-5 h of experiments were fitted to a pseudo first-order kinetics:

$$312 \quad [Diclof] = [Diclof]_0 \beta \exp\left(-k_1 t + \frac{1-\beta}{\beta}\right) \quad (9)$$

313 and

$$314 \quad TOC = TOC_0 \beta \exp\left(-k'_1 t + \frac{1-\beta}{\beta}\right) \quad (10)$$

315 where $[Diclof]_0$ and $[Diclof]$ are the initial and time-dependent concentrations of diclofenac; k_o
 316 and k_1 correspond to the zero-order and first-order rate constants for diclofenac oxidation; TOC and
 317 TOC_0 are the initial and time-dependent TOCs; k'_0 and k'_1 refer to the zero-order and first-order rate
 318 constants for TOC removal; and β is a dimensionless parameter depending on the applied and
 319 limiting current densities and the initial current efficiency, and reflects the condition at which the
 320 change from pseudo-zero to pseudo-first order regime occurs [34]. The plots of $[Diclof]$ or
 321 $\ln[Diclof]$ versus time were successfully fitted into straight lines with $R^2 > 0.99$ for all the studied
 322 anodes, thus, validating the application of the kinetic models. The rate constants were calculated
 323 from the slopes of these linear fittings and collected in Table 1.

324 Figure 5 shows that, as expected, BDD was the best anode to oxidize and mineralize diclofenac. This
 325 electrode reduced 100 % of diclofenac and 87 % of TOC in only 1 h, and enabled to reduce 100 %
 326 TOC in less than 3 h. These results agree with the extraordinary performance shown by this electrode
 327 to mineralize several organic pollutants [23-26,43-46]. Although it has been proved that it can
 328 directly oxidize diclofenac (section 3.1), the superior performance of BDD during electrolysis is
 329 mainly attributed to its facility to rapidly generate a large amount of highly oxidizing \cdot OHs (section
 330 3.2). In fact, the high potential of BDD during the electrolysis (+3.7 V vs. Ag/AgCl/Cl⁻(3.5 M),
 331 average, see Table S1) may guarantee the generation of an enormous amount \cdot OHs for such a fast

332 diclofenac electro-oxidation. Accordingly, the calculated rate constants for diclofenac oxidation and
333 mineralization were remarkably higher compared to the other electrodes tested (Table 1). By
334 contrast, Ti/Pt oxidized the 70 % of diclofenac and eliminated the 33 % of TOC in 5 h, presenting
335 the slowest reaction kinetics (Table 1) and, overall, the worst performance among the studied anodes.
336 This is in line with the poor activity of this anode for diclofenac oxidation observed by cyclic
337 voltammetry and the slowest kinetics for producing $\cdot\text{OHs}$ (Table 1). It can be inferred, then, that this
338 electrode working at +2.6 V vs. Ag/AgCl/Cl⁻(3 M) (average) promoted the OER during the
339 electrolytic experiment.

340 Regarding the SnO₂-Sb anodes, the performance of the SnO₂-Sb without Pt was found better than
341 that of Ti/Pt. The faster reaction kinetics on this anode (Table 1) resulted in 83 % of diclofenac
342 oxidation and ca. 40 % of TOC removal after 5 h treatment. This better response can be assigned to
343 the faster formation of $\cdot\text{OHs}$ (Table 1) and/or their higher oxidizing power when they are produced
344 on this non-active material (working at 2.65 V vs. Ag/AgCl/Cl⁻(3 M)).

345 Figure 5 demonstrates that the introduction of Pt improves the electro-oxidative response of the
346 Ti/SnO₂-Sb anode under galvanostatic conditions. Thus, with the introduction of 3 and 13 at.% Pt,
347 the diclofenac oxidation efficiency increases up to 89 and 91 %, respectively, and that for TOC
348 removal reaches relatively high values of ca. 53 and 61 %, respectively. Similar trends were found
349 for the values of the mineralization current efficiencies for the different anodes (for example, see
350 those calculated at 2 h provided in Table 1), remarking the intermediate performance of Ti/SnO₂-Sb-
351 Pt anodes between those of expensive commercial anodes.

352 The effect of Pt on the electrocatalytic response of Ti/SnO₂-Sb anodes found for diclofenac oxidation
353 has many similarities with that previously observed for phenol [33-35]. Independently of the
354 electrolyte, in both cases Pt improves the direct (non- $\cdot\text{OHs}$ -mediated) oxidation of the pollutant prior
355 OER and the pollutant removal by galvanostatic treatment, at least up to 3 % Pt. However, important
356 differences can be found too, especially for galvanostatic treatments. First, in H₂SO₄ the electrode

357 with the highest amount of Pt (Ti/SnO₂-Sb-Pt (13%)) showed the lowest activity for phenol oxidation
358 and mineralization [33], but it is the best one for the case of diclofenac in Na₂SO₄ (Fig. 5). Second,
359 phenol and diclofenac in basic [34] and neutral medium (Fig. 5), respectively, have exhibited a
360 change from pseudo-zero to pseudo-first order kinetics, while phenol in acid electrolyte showed a
361 first-order regime during the whole electrolytic treatment, even for initial concentrations as high as
362 1000 ppm [33]. These varying results and effects may be explained by the relative contribution of the
363 different processes involved, such as the pollutant-surface interaction/oxidation and the $\cdot\text{OH}$
364 generation, at which the structure of the pollutant and the pH of the medium may play a relevant role.
365 To explain the influence of Pt on the electro-oxidation of phenol in alkaline conditions, the specific
366 adsorption of phenolate ions on Pt/PtO_x was proposed to facilitate their reaction with highly
367 oxidizing $\cdot\text{OH}$ s formed on the SnO₂-Sb matrix [35]. However, the distinct rate for $\cdot\text{OH}$ s generation
368 was not studied. Interestingly, the present work demonstrates that Pt incorporation slows down the
369 rate for $\cdot\text{OH}$ s generation in neutral medium (Table 1). Then, the better response of these electrodes
370 for diclofenac removal can be attributed to the promoted interaction of diclofenac with surface Pt
371 species (observed by cyclic voltammetry, section 3.1), which could be even stronger than that with
372 phenolate. In fact, previous studies on the electrochemical behavior of organic acids on Pt surfaces
373 demonstrated a strong interaction and/or adsorption of these molecules through their carboxylic
374 group [52,53]. Hence, it is hypothesized that the superior performance of Pt-doped SnO₂-Sb anodes
375 towards diclofenac oxidation may be due to a strong interaction of diclofenac with Pt facilitated by
376 the carboxylic group in this pollutant. Nevertheless, it is noteworthy to remark that all these
377 hypotheses are based on the observation of voltammetric experiments and/or indirectly deduced from
378 performance parameters, so that the use of additional or coupled powerful techniques are necessary
379 to provide stronger evidences.

380

381 **4. Conclusions**

382 The voltammetric and galvanostatic study presented in this work demonstrates that Ti/SnO₂-Sb
383 anodes, with or without Pt, can efficiently oxidize and mineralize diclofenac. The good performance
384 of these electrodes has been voltammetrically observed at potentials below the OER, where they can
385 directly oxidize diclofenac, as well as at high potentials during electrolysis experiments, where the
386 oxidation is mainly mediated by hydroxyl radicals concurrently to the OER.

387 The calculated voltammetric oxidation charges, and the efficiencies and rate constants for diclofenac
388 oxidation and TOC removal indicate that the incorporation of small amounts of Pt (3-13 at.%)
389 remarkably enhances the performance of Ti/SnO₂-Sb anodes for diclofenac abatement (apart from
390 other benefits, such as an enhanced service life [31,32]). Interestingly, this electrocatalytic effect on
391 diclofenac removal is observed even though the Pt doping partly hinders the generation of [•]OHs,
392 what supposes a completely new finding that contradicts what would be expected from the literature.
393 From the observed strong interaction and good oxidation activity of diclofenac on polycrystalline Pt,
394 the enhanced response of Pt-doped Ti/SnO₂-Sb anodes is assigned to an effective Pt-diclofenac
395 interaction that may promote its oxidation directly and/or with the electrogenerated [•]OHs.

396 Comparisons with commercial anodes under similar experimental conditions show that the
397 performance of the Ti/SnO₂-Sb anodes lies in between those of Ti/Pt and BDD. The obtained results,
398 hence, enable to propose Pt-doped Ti/SnO₂-Sb anodes as potential cheaper alternatives to BDD for
399 the elimination of pharmaceuticals in wastewater.

400

401 **Acknowledgements**

402 The authors thank the Spanish Ministerio de Economía y Competitividad (MINECO) and FEDER
403 funds (grants MAT2016-76595-R and RYC-2017-23618) and Generalitat Valenciana (grant
404 PROMETEO/2018/087) for financial support.

405 **References**

406 [1] R. Altman, B. Bosch, K. Brune, P. Patrignani, C. Young. Advances in NSAID development: evolution of
407 diclofenac products using pharmaceutical technology. *Drugs* 75 (2015) 859-877.

- 408 [2] P. Verlicchi, A. Galletti, M. Petrovic, D. Barcelo. D. Hospital effluents as a source of emerging pollutants:
409 An overview of micropollutants and sustainable treatment options. *J. Hydrology* 389 (2010) 416-428.
- 410 [3] H. Yu, E. Nie, J. Xu, S. Yan, W.J. Cooper, W. Song. Degradation of Diclofenac by Advanced Oxidation
411 and Reduction Processes: Kinetic Studies, Degradation Pathways and Toxicity Assessments. *Water Res.* 47
412 (2013) 1909-1918.
- 413 [4] D.W. Kolpin, E.T. Furlong, M.T. Meyer, E.M. Thurman, S.D. Zaugg, L.B. Barber, H.T. Buxton.
414 Pharmaceuticals, Hormones, and Other Organic Wastewater Contaminants in U.S. Streams, 1999-2000: A
415 National Reconnaissance. *Environ. Sci. Technol.* 36 (2002) 1202-1211.
- 416 [5] J.H. Al-Rifai, C.L. Gabelish, A.I. Schafer. Occurrence of pharmaceutically active and non-steroidal
417 estrogenic compounds in three different wastewater recycling schemes in Australia. *Chemosphere* 69 (2007)
418 803-815.
- 419 [6] D. Stülten, S. Zühlke, M. Lamshöft, M. Spiteller. Occurrence of diclofenac and selected metabolites in
420 sewage effluents. *Sci. Total Environ.* 405 (2008) 310-316.
- 421 [7] H.-R. Buser, T. Poiger, M.D. Muller. Occurrence and Fate of the Pharmaceutical Drug Diclofenac in
422 Surface Waters: Rapid Photodegradation in a Lake. *Environ. Sci. Technol.* 32 (1998) 3449-3456.
- 423 [8] R. Triebkorn, H. Casper, A. Heyd, R. Eikemper, H.R. Köhler, J. Schwaiger. Toxic effects of the non-
424 steroidal antiinflammatory drug diclofenac Part II. Cytological effects in liver, kidney, gills and intestine of
425 rainbow trout (*Oncorhynchus mykiss*). *Aquat. Toxicol.* 68 (2004) 151-166.
- 426 [9] W.C. Maddrey. Clinical Manifestations and Management of Drug-Induced Liver Diseases, in *Drug-
427 Induced Liver Disease (Third Edition)* 2013, pp. 229-240.
- 428 [10] H. Krum, G. Swergold, A. Gammaitoni, P.M. Peloso, S.S. Smugar, S.P. Curtis, D.C. Brater, H. Wang, A.
429 Kaur, L. Laine, M.R. Weir, C.P. Cannon. Blood pressure and cardiovascular outcomes in patients taking
430 nonsteroidal antiinflammatory drugs. *Cardiovasc Ther.* 30 (2012) 342-350.
- 431 [11] J.L. Oaks, M. Gilbert, M.Z. Virani, R.T. Watson, C.U. Meteyer, B.A. Rideout, H.L. Shivaprasad, S.
432 Ahmed, M. Chaudhry, M. Arshad, S. Mahmood, A. Ali, A. A. Khan,. Diclofenac residues as the cause of
433 vulture population decline in Pakistan. *Nature* 427 (2004) 630-633.
- 434 [12] B. Silva, F. Costa, I.C. Neves, T. Tavares. Psychiatric Pharmaceuticals as Emerging Contaminants in
435 Wastewater. *SpringerBriefs in Green Chemistry for Sustainability*.
- 436 [13] T. Heberer. Occurrence, fate, and removal of pharmaceutical residues in the aquatic environment: a
437 review of recent research data. *Toxicol. Lett.* 131 (2002) 5-17.
- 438 [14] X. Yang, R.C. Flowers, H.S. Weinberg, P.C. Singer, Occurrence and removal of pharmaceuticals and
439 personal care products (PPCPs) in an advanced wastewater reclamation plant, *Water Res.* 45 (2011) 5218-
440 5228
- 441 [15] J. Rivera-Utrilla, M. Sánchez-Polo, M.A. Ferro-García, G. Prados-Joya, R. Ocampo-Pérez.
442 Pharmaceuticals as emerging contaminants and their removal from water. A review. *Chemosphere* 93 (2013)
443 1268-1287
- 444 [16] O.M. Rodriguez-Narvaez, J.M. Peralta-Hernandez, A. Goonetilleke, E.R. Bandala. Treatment
445 technologies for emerging contaminants in water: A review. *Chem. Eng. J.* 323 (2017) 361-380
- 446 [17] Ch. Comninellis. Electrocatalysis in the electrochemical conversion/combustion of organic pollutants for
447 waste water treatment. *Electrochim. Acta* 39 (1994) 1857-1862.

- 448 [18] C.A. Martínez-Huitle, S. Ferro. Electrochemical oxidation of organic pollutants for the wastewater
449 treatment: Direct and indirect processes. *Chem. Soc. Rev.* 25 (2006) 1324-1340.
- 450 [19] M. Panizza, G. Cerisola, Direct And Mediated Anodic Oxidation of Organic Pollutants. *Chem. Rev.* 109
451 (2009) 6541–6569.
- 452 [20] A. Kapałka, G. Fóti, Ch. Comninellis. Basic Principles of the Electrochemical Mineralization of Organic
453 Pollutants for Wastewater Treatment, in: Ch. Comninellis, G. Chen (Eds.), *Electrochemistry for the*
454 *Environment*, Springer, New York, 2010, pp. 1-23.
- 455 [21] I. Sirés, E. Brillas. Remediation of water pollution caused by pharmaceutical residues based on
456 electrochemical separation and degradation technologies: A review. *Environ. Int.* 45 (2012) 212-229.
- 457 [22] K. Rajeshwar, J.G. Ibanez, *Environmental Electrochemistry: Fundamentals and Applications in Pollution*
458 *Abatement*, Academic Press Inc., San Diego, 1997.
- 459 [23] A. Kapałka, G. Fóti, and C. Comninellis. The importance of electrode material in environmental
460 electrochemistry: formation and reactivity of free hydroxyl radicals on boron-doped diamond electrodes.
461 *Electrochim. Acta* 54 (2009) 2018-2023.
- 462 [24] X. Zhao, Y. Hou, H. Liu, Z. Qiang, J. Qu. Electro-oxidation of diclofenac at boron doped diamond:
463 kinetics and mechanism. *Electrochim. Acta* 54 (2009) 4172-4179.
- 464 [25] E. Brillas, S. Garcia-Segura, M. Skoumal, C. Arias, Electrochemical incineration of diclofenac in neutral
465 aqueous medium by anodic oxidation using Pt and boron-doped diamond anodes. *Chemosphere* 79 (2010)
466 605-612.
- 467 [26] M.D. Vedenyapina, D.A. Borisova, K.-H. Rosenwinkel, D. Weichgrebe, P. Stopp, A.A. Vedenyapin.
468 Kinetics and Mechanism of the Deep Electrochemical Oxidation of Sodium Diclofenac on a Boron-Doped
469 Diamond. *Russian J. Phys. Chem. A* 87 (2013) 1393–1396.
- 470 [27] Z. Ji, T. Liu, H. Tian. Electrochemical degradation of diclofenac for pharmaceutical wastewater
471 treatment. *Int. J. Electrochem. Sci.* 12 (2017) 7807-7816.
- 472 [28] F.W. Sifuna, F. Orata, V. Okello, S. Jemutai-Kimosop. Comparative studies in electrochemical
473 degradation of sulfamethoxazole and diclofenac in water by using various electrodes and phosphate and
474 sulfate supporting electrolytes. *J. Environ. Sci. Health A Tox. Hazard. Subst. Environ. Eng.* 51 (2016) 954-
475 961.
- 476 [29] C. Comninellis, C. Pulgarin, Electrochemical oxidation of phenol for wastewater treatment using SnO₂
477 anodes. *J. Appl. Electrochem.* 23 (1993) 108–112
- 478 [30] S. Stucki, R. Kotz, B. Carcer, W. Suter. Electrochemical waste water treatment using high overvoltage
479 anodes Part II: Anode performance and applications. *J. Appl. Electrochem.* 21 (1991) 99-104.
- 480 [31] F. Montilla, E. Morallón, A. De Battisti, J.L. Vázquez. Preparation and Characterization of Antimony-
481 Doped Tin Dioxide Electrodes. Part 1. Electrochemical Characterization *J. Phys. Chem. B* 108 (2004) 5036-
482 5043.
- 483 [32] R. Berenguer, J.M. Sieben, C. Quijada, E. Morallón. Pt- and Ru-Doped SnO₂-Sb Anodes with High
484 Stability in Alkaline Medium. *ACS Appl. Mater. Interf.* 6 (2014) 22778-22789.
- 485 [33] F. Montilla, E. Morallón, J.L. Vázquez. Evaluation of the Electrocatalytic Activity of Antimony-Doped
486 Tin Dioxide Anodes toward the Oxidation of Phenol in Aqueous Solutions *J. Electrochem. Soc.* 152 (2005)
487 B421.

- 488 [34] R. Berenguer, J.M. Sieben, C. Quijada, E. Morallón. Electrocatalytic degradation of phenol on Pt- and
489 Ru-doped Ti/SnO₂-Sb anodes in an alkaline medium. *Appl. Catal. B: Environ.* 199 (2016) 394-404.
- 490 [35] R. Berenguer, C. Quijada, E. Morallón. The Nature of the Electro-Oxidative Catalytic Response of Mixed
491 Metal Oxides: Pt- and Ru-Doped SnO₂ Anodes. *ChemElectroChem* 6 (2019) 1-14.
- 492 [36] R. Berenguer, C. Quijada, E. Morallón. Electrochemical Characterization of SnO₂ Electrodes Doped with
493 Ru and Pt. *Electrochim. Acta* 54 (2009) 5230-5238.
- 494 [37] F. Montilla, E. Morallón, A. De Battisti, A. Benedetti, H. Yamashita, J.L. Vázquez. Preparation and
495 Characterization of Antimony-Doped Tin Dioxide Electrodes. Part 2. XRD and EXAFS Characterization *J.*
496 *Phys. Chem. B* 104 (2004) 5044-5050.
- 497 [38] F. Montilla, E. Morallón, A. De Battisti, S. Barison, S. Daolio, J.L. Vázquez. Preparation and
498 Characterization of Antimony-Doped Tin Dioxide Electrodes. 3. XPS and SIMS Characterization. *J. Phys.*
499 *Chem. B* 108 (2004) 15976-15981.
- 500 [39] A. Wieckowski. *Interfacial Electrochemistry: Theory, Experiment, and Applications*. CRC Press: New
501 York, USA, 1999.
- 502 [40] M.O. Pacheco-Álvarez, O.M. Rodríguez-Narváez, K. Wrobel, R. Navarro-Mendoza, J.L. Nava-Montes
503 de Oca, J.M Peralta-Hernández. Improvement of the Degradation of Methyl Orange Using a TiO₂/BDD
504 Composite Electrode to Promote Electrochemical and Photoelectro-Oxidation Processes. *Int. J. Electrochem.*
505 *Sci.* 13 (2018) 11549-11567.
- 506 [41] Z.G. Aguilar, O. Coreño, M. Salazar, I. Sirés, E. Brillas, J.L. Nava. Ti|Ir-Sn-Sb oxide anode: Service life
507 and role of the acid sites content during water oxidation to hydroxyl radicals. *J. Electroanal. Chem.*, 820
508 (2018) 82-88.
- 509 [42] M.I. León, Z.G. Aguilar, J.L. Nava. Electrochemical combustion of indigo at ternary oxide coated
510 titanium anodes. *J. Electrochem. Sci. Eng.* 4 (2014) 247-258.
- 511 [43] P. Cañizares, F. Martínez, M. Díaz, J. García-Gómez, M.A. Rodrigo, Electrochemical Oxidation of
512 Aqueous Phenol Wastes Using Active and Nonactive Electrodes. *Water Res.* 39 (2005) 2687-2703.
- 513 [44] M.A. Rodrigo, P.A. Michaud, I. Duo, M. Panizza, G. Cerisola, Ch. Comninellis, Oxidation of 4-
514 Chlorophenol at Boron-Doped Diamond Electrode for Wastewater Treatment. *J. Electrochem. Soc.* 148
515 (2001) D60-D64.
- 516 [45] M. Panizza, P.A. Michaud, G. Cerisola, Ch. Comninellis. Anodic oxidation of 2-naphthol at boron-doped
517 diamond electrodes. *J. Electroanal. Chem.* 507 (2001) 206-214.
- 518 [46] B. Marselli, J. Garcia-Gomez, P.-A. Michaud, M.A. Rodrigo, Ch. Comninellis. Electrogeneration of
519 Hydroxyl Radicals on Boron-Doped Diamond Electrodes. *J. Electrochem. Soc.* 150 (2003) D79-D83.
- 520 [47] O. Scialdone, S. Randazzo, A. Galia, G. Filardo. Electrochemical oxidation of organics at metal oxide
521 electrodes: The incineration of oxalic acid at IrO₂-Ta₂O₅ (DSA-O₂) anode. *Electrochim. Acta* 54 (2009)
522 1210-1217.
- 523 [48] O. Scialdone. Electrochemical oxidation of organic pollutants in water at metal oxide electrodes: A
524 simple theoretical model including direct and indirect oxidation processes at the anodic surface.
525 *Electrochim. Acta* 54 (2009) 6140-6147.
- 526 [49] O. Scialdone, S. Randazzo, A. Galia, G. Silvestri. Electrochemical oxidation of organics in water: Role of
527 operative parameters in the absence and in the presence of NaCl. *Water Res.* 43 (2009) 2260-2272.

- 528 [50] W. Vielstich, H. A. Gasteiger, H. Yokokawa. Handbook of Fuel Cells: Advances in Electrocatalysis,
529 Materials, Diagnostics and Durability. John Wiley & Sons (2009).
- 530 [51] Ch. Comninellis, C. Pulgarin. Anodic oxidation of phenol for waste water treatment. J. Appl.
531 Electrochem. 21 (1991) 703-708.
- 532 [52] F. Huerta, E. Morallón, F. Cases, A. Rodes, J.L. Vázquez, A. Aldaz. Electrochemical behaviour of amino
533 acids on Pt(h,k,l): a voltammetric and in situ FTIR study. Part 1. Glycine on Pt(111). J. Electroanal. Chem.
534 421 (1997) 179-185.
- 535 [53] F. Montilla, E. Morallón, J.L. Vázquez. Electrochemical Behaviour of Benzoic Acid on Platinum and
536 Gold Electrodes. Langmuir 19 (2003) 10241-10246.

Journal Pre-proof

Supporting Information

Generation of Hydroxyl Radicals and Electro-oxidation of Diclofenac on Pt-doped SnO₂-Sb electrodes

Maribel Fernández^{a,b}, Raúl Berenguer^a, Samuel Beaumont^a, Montserrat Nuez^a, Adolfo La Rosa-Toro^b, Juan Manuel Peralta-Hernández^c, Emilia Morallón^a

^a Instituto Universitario de Materiales and Departamento de Química Física. Universidad de Alicante. Apartado 99. E-03080 Alicante (Spain)

^b Escuela Profesional de Química, Facultad de Ciencias, Universidad Nacional de Ingeniería, Av. Túpac Amaru, 210, Lima (Peru)

^c Departament of Chemistry, Universidad de Guanajuato (Mexico)

Corresponding author
raul.berenguer@ua.es

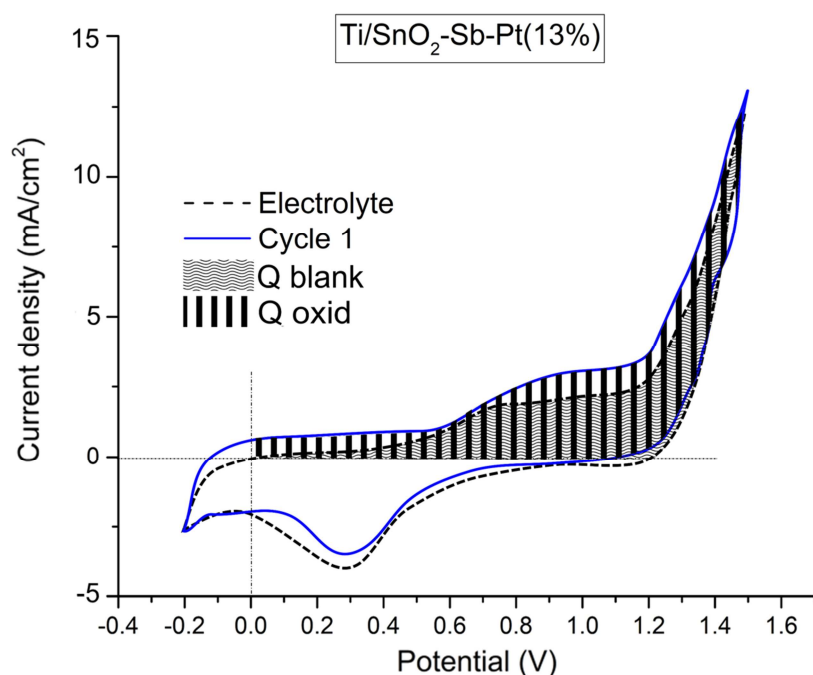


Figure S1. Voltammetric areas integrated for the calculation of the charge associated to diclofenac oxidation prior the OER (Q_{oxid}/Q_{blank}). Example for the Ti/SnO₂-Sb-Pt(13%) anode.

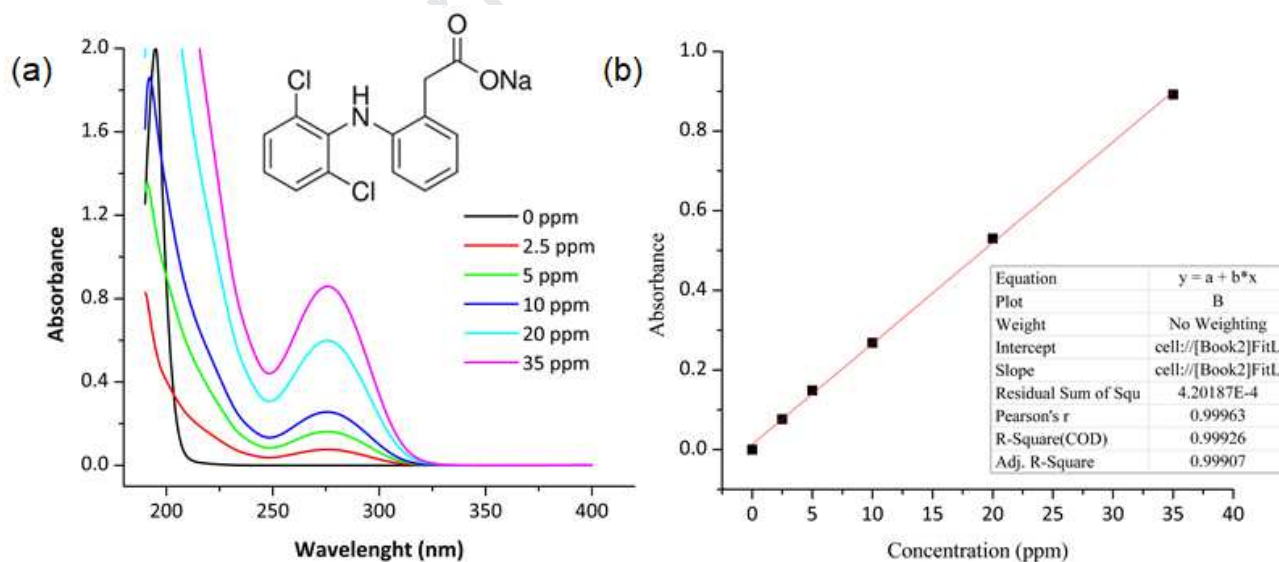


Figure S2. (a) UV spectra of 0.5 M Na₂SO₄ aqueous solutions with different sodium diclofenac concentrations; and (b) the calibration curve for spectroscopic determination of diclofenac.

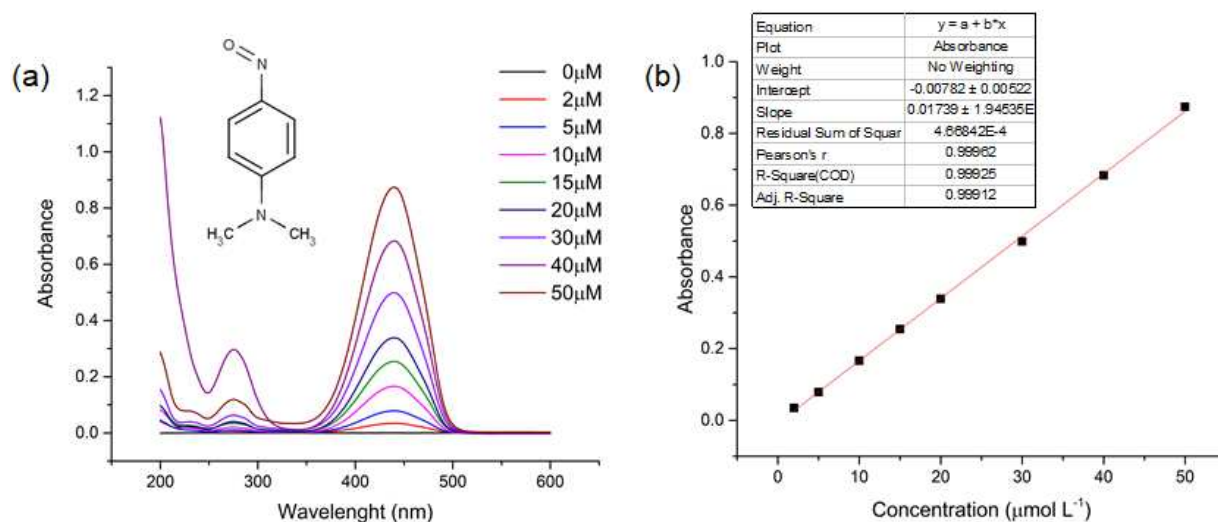


Figure S3. (a) UV spectra of differently concentrated RNO solutions; and the (b) calibration curve for spectroscopic determination of RNO.

Electrochemical behavior of diclofenac on polycrystalline Pt studied by cyclic voltammetry

Figure S4 shows the response of a polycrystalline Pt electrode, used as model reference material, in the absence and presence of diclofenac. In the absence of diclofenac (black dash line), the voltammogram presents the characteristic hydrogen adsorption-desorption and reduction-oxidation peaks (H_a , H_d) as well as the Pt surface oxidation-reduction (Pt_{ox} , $PtOx_{red}$) processes [1].

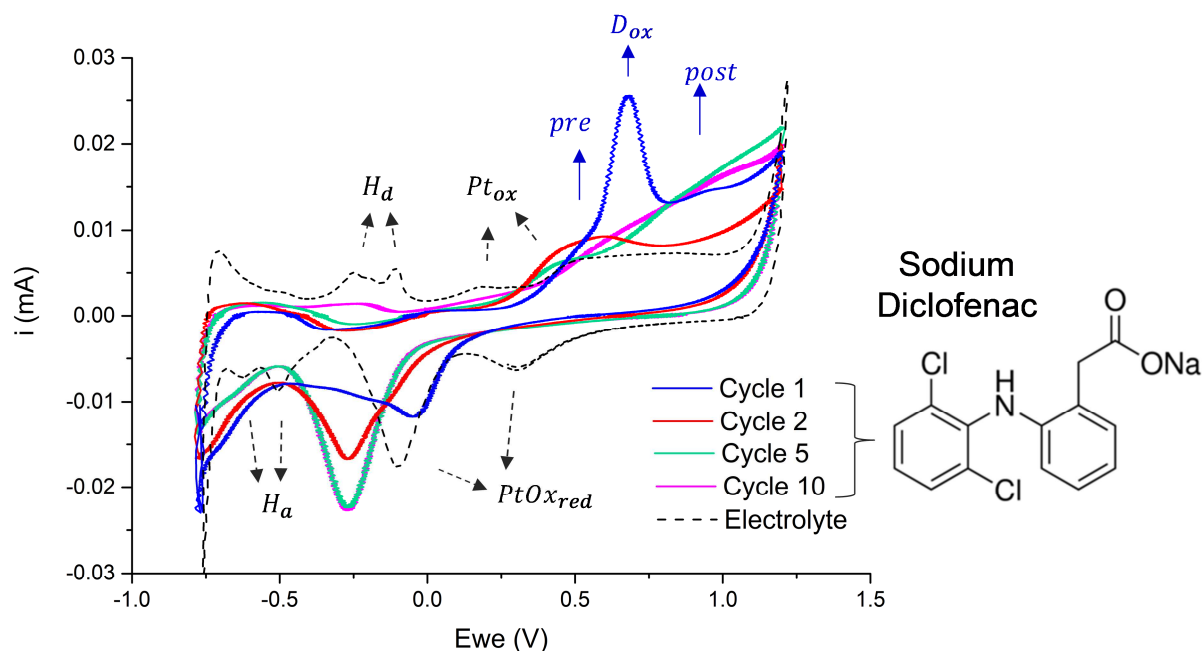


Figure S4. Successive cyclic voltammograms of a polycrystalline Pt electrode in 200 ppm diclofenac + 0.5 M Na_2SO_4 aqueous solution. Scan rate = 50 mV s^{-1} . Reference electrode $\text{Ag}/\text{AgCl}/3\text{M KCl}$.

In the presence of diclofenac (blue rigid line), however, the electrode shows a reduced current and no oxidation processes during the first forward cycle from -0.8 to 0.25 V. This suggests the adsorption of diclofenac on the Pt surface within this potential range. From 0.25 V, the anodic current rises and a defined oxidation peak (D_{ox}) centred at 0.68 V is clearly observed in the first cycle. Moreover, the overlapped processes before and after the peak (*pre* and *post*, respectively) are indicative of other concurrent oxidation processes. These processes are assigned to the non- \cdot OH-mediated oxidation of adsorbed and/or solution diclofenac and derived oxidation by-products on Pt and/or PtOx surfaces.

During the reverse cathodic scan, the peaks attributed to reduction of surface PtOx species, centred at 0.32 V and -0.11 V, are remarkably affected, and only one cathodic peak of intermediate intensity and potential (at ca. -0.05 V) is observed. Similar effects were found with other organic compounds [2]. These effects may be assigned to changes in the pH (acidification), in the proximity of the electrode surface, during the positive scan as a consequence of the OER. This local acidity might also promote diclofenac protonation, affecting the chemistry of electroactive species. Nevertheless, this local acidification may be partly compensated by cathodic processes (hydrogen evolution reaction) during the reverse scan. On the one hand, these voltammetric changes could also indicate that the oxidation of surface Pt to PtOx during the forward cycle is influenced by concurrent diclofenac oxidation, and/or that the oxidation products cause an effect on the reduction process. In this sense, a progressive change on the electrochemical response of the Pt electrode was observed during the second and successive cycles (red and green rigid lines).

Particularly, the anodic peak at 0.68 V practically disappears in the 2nd cycle; the pre-oxidation process becomes important in the 2nd and subsequently vanishes upon cycling; and the relative intensity of the post-oxidation processes between 0.90 and 1.20 V increases. Moreover, the cathodic peak further shifts to -0.26 V and its intensity progressively increases with the number of cycles. All these observations reflected a significant interaction and effective oxidation of diclofenac and by-products on Pt, making it a promising dopant for diclofenac oxidation.

Differences in the electrocatalytic activity of the distinct Pt electrodes studied in this work

This work shows the electrochemical response of three different types of electrodes involving or containing Pt, namely Pt-doped Ti/SnO₂-Sb anodes (target) and polycrystalline Pt and Ti/Pt (for comparison purposes), and they exhibit quite different response towards diclofenac oxidation. This is quite normal and expected, since it is well known that the electrocatalytic activity of Pt catalysts is very sensitive to many factors, highlighting surface cleanliness, defects and arrangement of Pt atoms; Pt crystalline planes; dimensions and morphology of Pt phases; dispersion and surface area, etc. [3-5]. All these characteristics of Pt are mainly determined by the nature of the precursor and the preparation and pre-treatment methods.

Accordingly, these electrodes have no similarity in response because they have been prepared and pre-treated by different methods:

- As explained in the experimental section, for the polycrystalline Pt electrode “Prior usage, the surface of this electrode was thermally annealed and cleaned and subsequently protected from the laboratory atmosphere by a droplet of ultrapure water ...” This thermal treatment is achieved by a blue flame at very high temperatures, enabling to obtain a completely clean Pt surface with a characteristic surface atoms arrangement. Such a clean electrode presents a highly active and easily reproducible electrochemical response that makes it a model electrocatalyst for fundamental studies.

- On the contrary, the Ti/Pt electrode is a commercial product prepared by electrochemical deposition of a thin film of Pt onto a Ti substrate. This constitutes the feasible Pt electrode for practical application and cannot be thermally cleaned or annealed by using the previous method, since the high-temperature flame would make Pt to react with Ti support. Instead, this electrode is cleaned electrochemically (see details in the experimental section), so that its different cleaning degree and/or atomic surface arrangement may make this electrode considerably less active than polycrystalline Pt.

- Finally, the physico-chemical properties of Pt-doped Ti/SnO₂-Sb electrodes, prepared by thermal decomposition of proper metallic salt precursors, have been reported in previous papers [6-10]. Briefly, in these electrodes Pt/PtOx nano-/submicron domains are uniformly spread out over a matrix of SnO₂-Sb. Although both electrodes are cleaned by a similar electrochemical pre-treatment, the distinct structure of Pt phase in the form of small particles surrounded by such an effective matrix for [•]OH generation may be responsible of the higher activity of Pt-doped Ti/SnO₂-Sb electrodes compared to Ti-supported bulk Pt films in Ti/Pt.

Table S1. Electrode potential of the different anodes and cell voltage reached during the 5h-galvanostatic oxidation of diclofenac at 50 mA cm^{-2} . Electrolyte (0.2 L) = 200 ppm diclofenac + 0.5 M Na_2SO_4 .

Electrode	E_{ANODE} (V vs. Ag/AgCl/3M KCl)	Voltage (V)
Ti/Pt	2.57-2.68	4.9
BDD	3.89-3.77	6.0
Ti/SnO ₂ -Sb	2.08-2.65	6.0-6.5
Ti/SnO ₂ -Sb-Pt(3%)	1.83-1.90	4.4
Ti/SnO ₂ -Sb-Pt(13%)	2.12-2.08	4.8

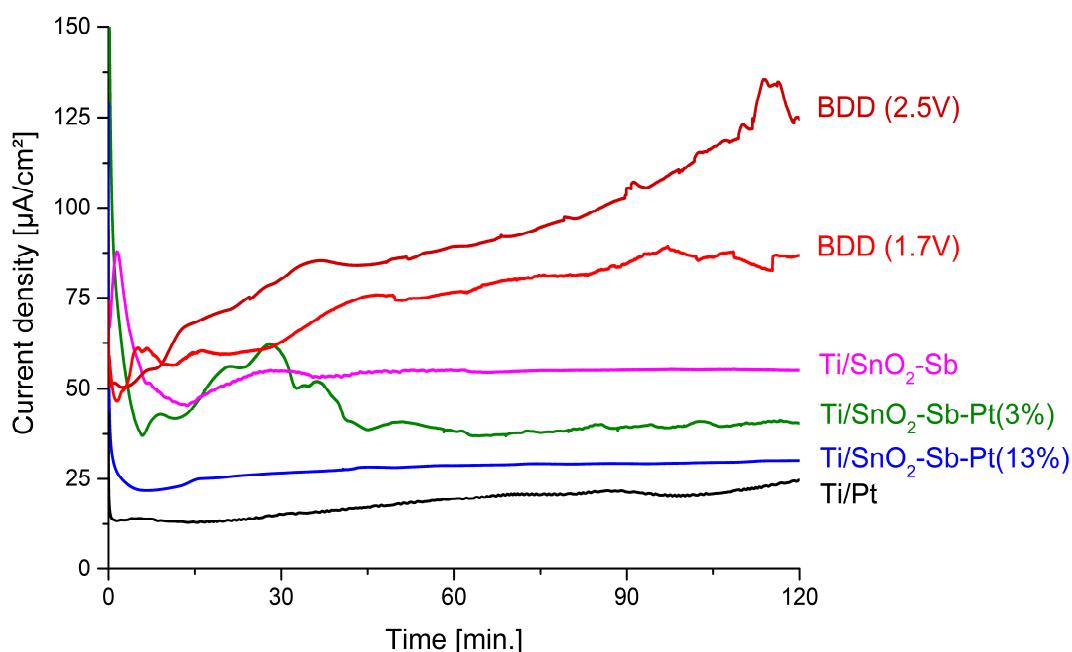


Figure S5. Evolution of current density during in-situ UV potentiostatic electrolysis of aqueous RNO solutions ($2 \times 10^{-5} \text{ mol dm}^{-3}$) with the different anodes at 1.7 V vs. Ag/AgCl/Cl⁻(3 M) and BDD at 2.4 V vs. Ag/AgCl/Cl⁻(3 M).

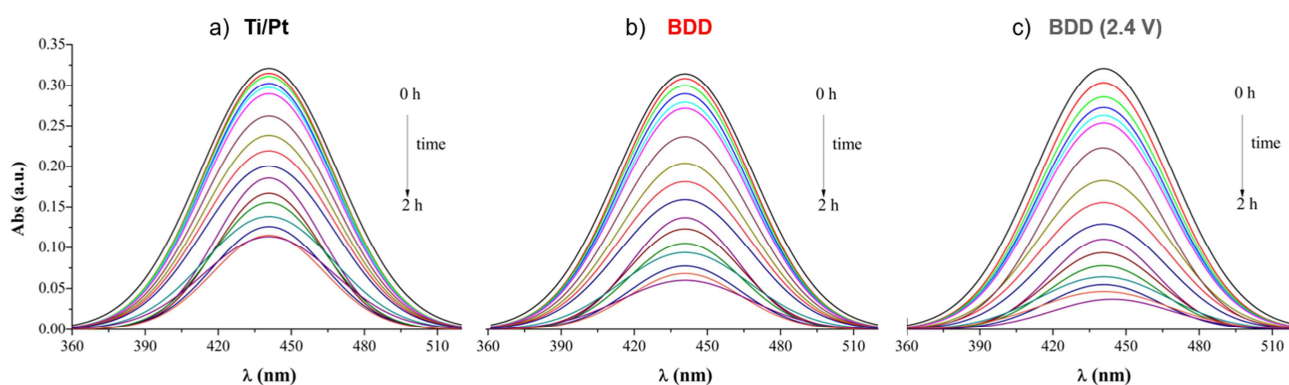


Figure S6. UV absorption spectra of aqueous RNO ($2 \times 10^{-5} \text{ mol dm}^{-3}$) obtained at 5 min intervals during 2 h potentiostatic electrolysis with (a) Ti/Pt and (b) BDD at 1.7 V vs. Ag/AgCl/Cl⁻ (3 M); and (c) BDD at 2.4 V vs. Ag/AgCl/Cl⁻ (3 M).

References

- [1] T. Konishi, M. Kiguchi, K. Murakoshi. Quantized conductance behavior of Pt metal nanoconstrictions under electrochemical potential control. *Surf. Sci.* 601 (2007) 4122-4126.
- [2] E. Wudarska, E. Chrzescijanska, E. Kusmierk, J. Rynkowski, Voltammetric studies of acetylsalicylic acid electrooxidation at platinum electrode, *Electrochim. Acta* 93 (2013) 189-194.
- [3] W. Vielstich, H. A. Gasteiger, H. Yokokawa. *Handbook of Fuel Cells: Advances in Electrocatalysis, Materials, Diagnostics and Durability.* John Wiley & Sons (2009).
- [4] M. Shao, Q. Chang, J.-P. Dodelet, R. Chenitz. Recent Advances in Electrocatalysts for Oxygen Reduction Reaction. *Chem. Rev.* 116 (2016) 3594-3657.
- [5] S. Sui, X. Wang, X. Zhou, Y. Su, S. Riffat, C.-J. Liu. A comprehensive review of Pt electrocatalysts for the oxygen reduction reaction: Nanostructure, activity, mechanism and carbon support in PEM fuel cells. *J. Mater. Chem. A*, 5 (2017) 1808-1825.
- [6] F. Montilla, E. Morallón, A. De Battisti, J.L. Vázquez. Preparation and Characterization of Antimony-Doped Tin Dioxide Electrodes. Part 1. Electrochemical Characterization *J. Phys. Chem. B* 108 (2004) 5036-5043.
- [7] F. Montilla, E. Morallón, A. De Battisti, A. Benedetti, H. Yamashita, J.L. Vázquez. Preparation and Characterization of Antimony-Doped Tin Dioxide Electrodes. Part 2. XRD and EXAFS Characterization *J. Phys. Chem. B* 104 (2004) 5044-5050.
- [8] F. Montilla, E. Morallón, A. De Battisti, S. Barison, S. Daolio, J. L. Vázquez. Preparation and Characterization of Antimony-Doped Tin Dioxide Electrodes. 3. XPS and SIMS Characterization. *J. Phys. Chem. B* 108 (2004) 15976-15981.
- [9] R. Berenguer, J.M. Sieben, C. Quijada, E. Morallón. Pt- and Ru-Doped SnO₂-Sb Anodes with High Stability in Alkaline Medium. *ACS Appl. Mater. Interf.* 6 (2014) 22778-22789.

[10] R. Berenguer, C. Quijada, E. Morallón. The Nature of the Electro-Oxidative Catalytic Response of Mixed Metal Oxides: Pt- and Ru-Doped SnO₂ Anodes. *ChemElectroChem* 6 (2019) 1-14.

Journal Pre-proof

Tables and Figures

Table 1. Effect of the anode on the voltammetric oxidation charge (Q_{oxid}/Q_{blank}); apparent rate constant for $\cdot OH$ generation ($k_{app}(\cdot OH)$) at 1.7 V (vs. Ag/AgCl/3M KCl); pseudo zero-order and first-order rate constants and 5 h-removal efficiencies for diclofenac oxidation (k_0, k_1) and TOC removal (k'_0, k'_1); and the mineralization current efficiency (MCE) at 2 h, in 0.5 M Na_2SO_4 .

Electrode	CV	$\cdot OH_s$	Diclofenac oxidation (UV)			TOC removal			
	Q_{oxid}/Q_{blank}	$k_{app}(\cdot OH)$ (min^{-1})	Eff_{Diclof} (%)	$10^8 k_0$ ($mol\ m^{-3}\ s^{-1}$)	$10^5 k_1$ (s^{-1})	Eff_{TOC} (%)	$10^4 k'_0$ ($mol\ m^{-3}\ s^{-1}$)	$10^5 k'_1$ (s^{-1})	MCE (%)
Ti/Pt	1.05	0.0088	70	5.34	6.12	33	8.49	1.00	2.7
BDD	20.8	0.0132/ 0.0161 ^a	100 ^b	41.2	80.9	100	25.56	71.40	9.9
Ti/SnO ₂ -Sb	1.45	0.0130	83	5.44	9.36	38	10.41	0.95	3.1
Ti/SnO ₂ -Sb-Pt(3%)	1.72	0.0113	90	7.29	11.7	53	12.32	1.96	4.0
Ti/SnO ₂ -Sb-Pt(13%)	1.76	0.0110	91	10.2	12.7	61	15.82	2.51	5.1

^a $k_{app}(\cdot OH)$ (min^{-1}) calculated at 2.4 V (vs. Ag/AgCl/3M KCl)

^b Eff_{Diclof} (%) after 1 h electrolysis

Figure 1. Scheme of (a) the electrochemical cell and (b) experimental set-up for the in-situ UV spectroelectrochemical measurements.

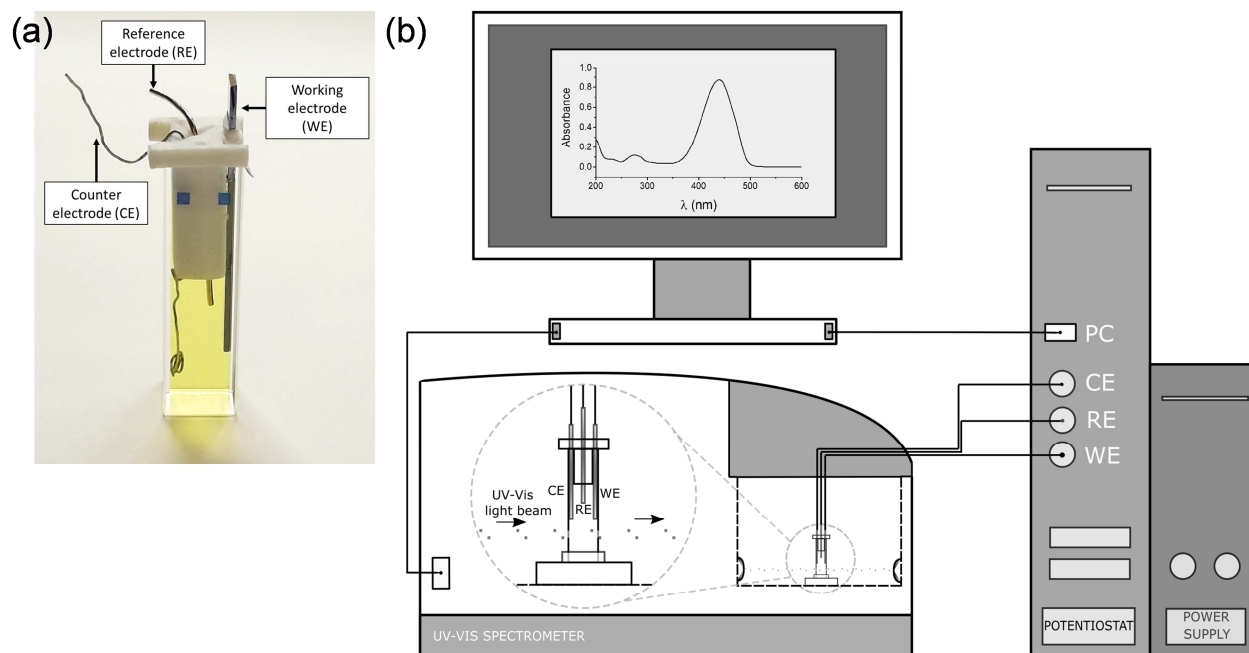


Figure 2. Cyclic voltammograms of (a) Ti/Pt and (b) BDD commercial anodes and those of (c-e) synthesized Ti/SnO₂-Sb-Pt(x) with x = 0 (c), 3 (d) and 13 (e) at.% Pt electrodes in the absence or presence of 200 ppm diclofenac. Electrolyte = 0.5 M Na₂SO₄. Reference electrode Ag/AgCl/3M KCl.

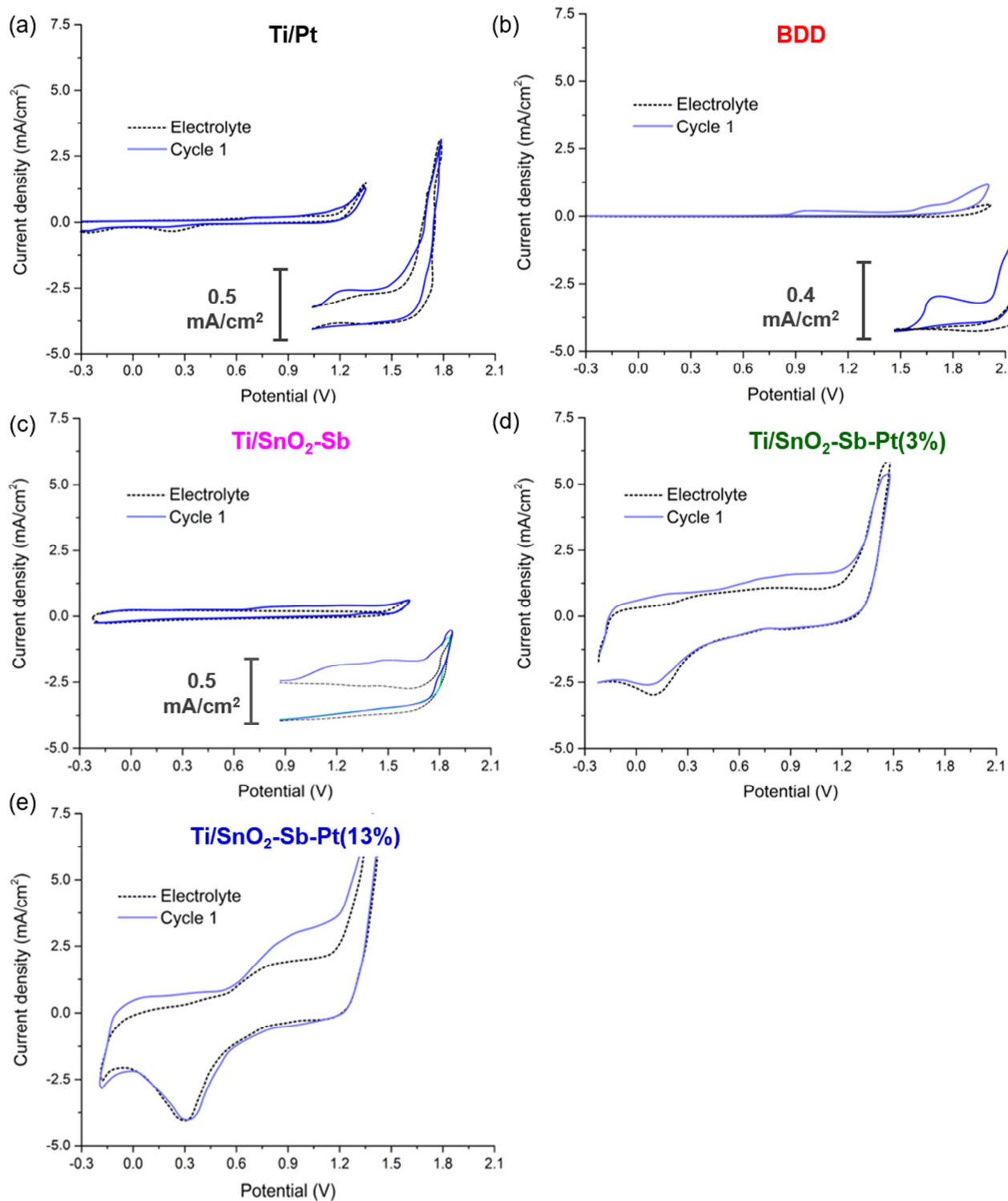


Figure 3. (a-c) UV absorption spectra of aqueous RNO (2×10^{-5} mol dm $^{-3}$) obtained at 5 min intervals during 2 h potentiostatic electrolysis with different SnO $_2$ -Sb anodes at 1.7 V (vs. Ag/AgCl/3M KCl); and (d) the pseudo-first order kinetics (linear plots) of RNO degradation for determination of the apparent rate constant (k_{app}) for \cdot OHs generation on the different anodes.

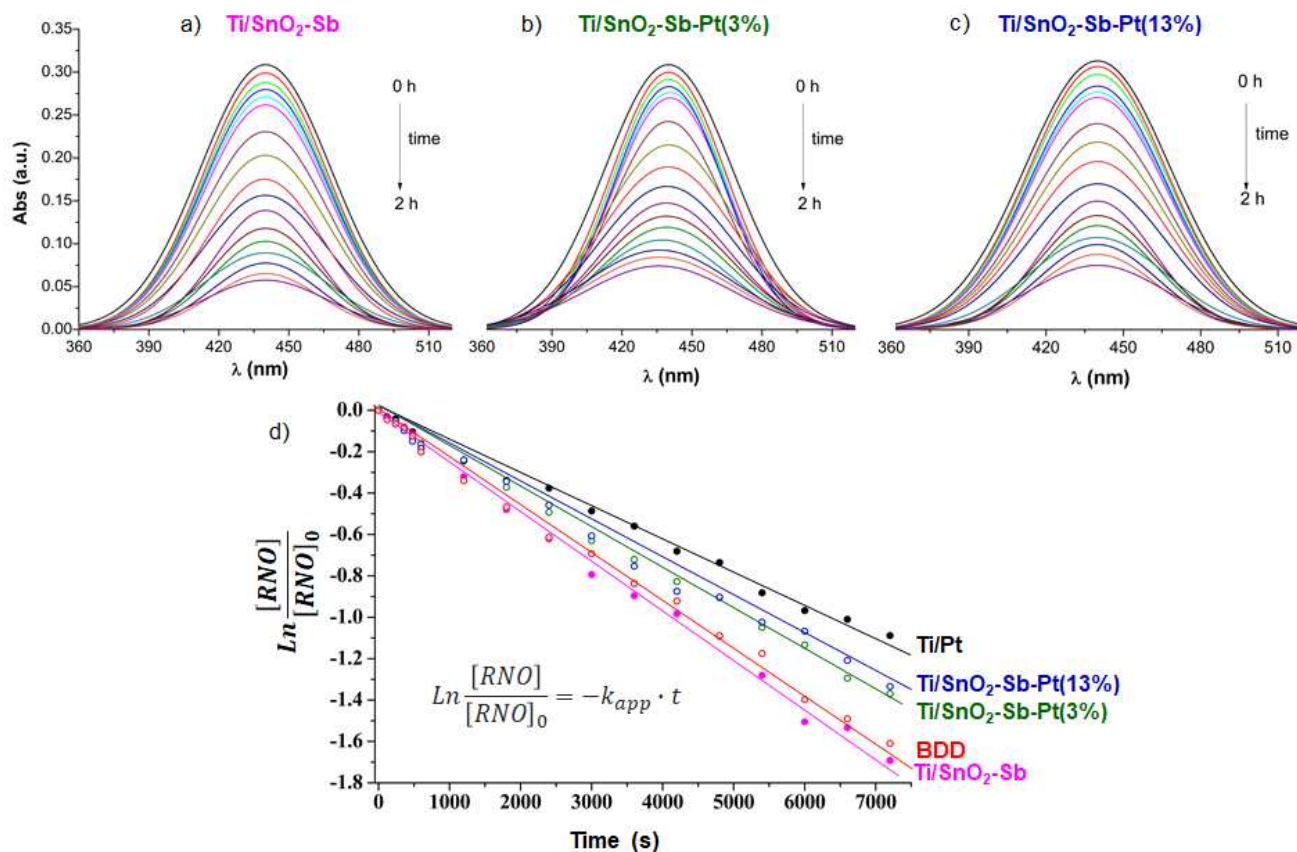


Figure 4. Evolution of diclofenac UV spectrum with time during the galvanostatic oxidation of a 200 ppm sodium diclofenac + 0.5 M Na₂SO₄ aqueous solution with different anodes. $j = 50 \text{ mA cm}^{-2}$.

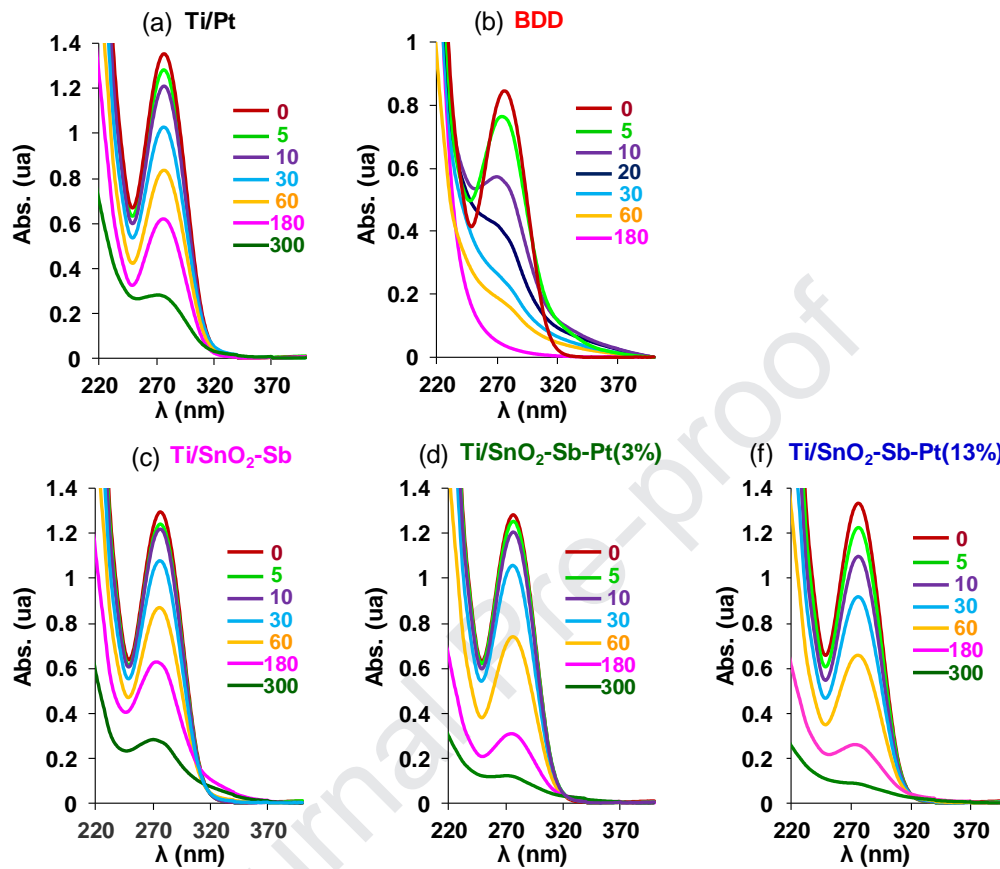
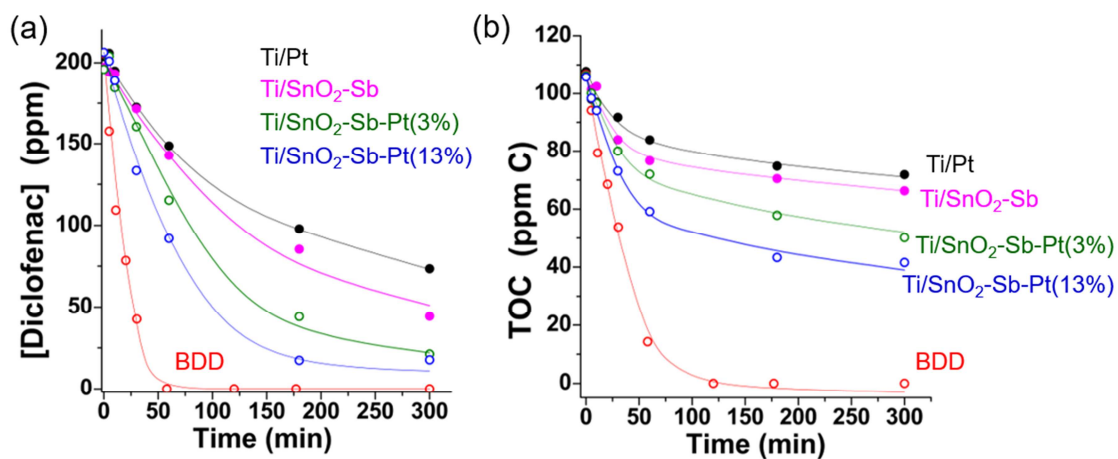


Figure 5. Evolution of the (a) diclofenac concentration (from UV) and (b) COT with time for the different anodes during the galvanostatic treatment at 50 mA cm^{-2} . Electrolyte = 200 ppm diclofenac + 0.5 M Na_2SO_4 .



Declaration of interests

The authors declare that they have no known competing financial interests or personal relationships that could have appeared to influence the work reported in this paper.

The authors declare the following financial interests/personal relationships which may be considered as potential competing interests: